Biochimica et Biophysica Acta, 645 (1981) 143–148

BBA 79250

^{31}P-NMR INVESTIGATIONS OF PHASE SEPARATION IN PHOSPHATIDYLCHOLINE/PHOSPHATIDYLETHANOLAMINE MIXTURES

KLAUS ARNOLD [a], ANDREAS LÖSCHE [b] and KLAUS GAWRISCH [b]

[a] *Sektion Biologie, Bereich Biophysik, Humboldt Universität, 104 Berlin (G.D.R.) and* [b] *Sektion Physik, Karl Marx Universität, 701 Leipzig (G.D.R.)*

(Received August 6th, 1980)
(Revised manuscript received February 16th, 1981)

Key words: ^{31}*P-NMR; Phase separation; Phosphatidylcholine; Phosphatidylethanolamine*

A phase diagram of DPPC-DPPE mixture is constructed by an analysis of the temperature dependence of the anisotropy of chemical shift of the ^{31}P-NMR signals of the individual components. At each temperature the phase state of the individual phospholipids is described. Thus ^{31}P-NMR is more informative than other methods such as ESR, DSC and fluorescence. The measurements confirm the conclusion of other authors that there is a phase separation in the gel state. In the temperature range of the phase transition the molecules are exchanged rapidly between liquid-crystalline and solid regions. In addition to the phase diagram a theoretical approach is applied to estimate the relative distribution of like and unlike molecules in the liquid-crystalline state and a nonrandom distribution is found.

I. Introduction

Phosphatidylcholine and phosphatidylethanolamine are major constituents of most cell membranes. Therefore it is important to characterize the physical properties of mixtures of these components. Studies of mixtures of the synthetic phospholipids dipalmitoyl phosphatidylcholine (DPPC) and dipalmitoyl phosphatidylethanolamine (DPPE) were performed using different methods, such as ESR [1], DSC [2], fluorescence [3] and ^{31}P-NMR [4]. These investigations appear to indicate immiscibility of these lipids in the solid phase and were discussed in terms of a separation of the lipids within the plane of the bilayer [5–7].

There have as yet been only few studies on the motional parameters of phospholipid-phospholipid mixtures [5]. In this study ^{31}P-NMR techniques were employed; they provide a convenient method for investigating both the polymorphic phase behaviour and the mobility of phospholipids [8–14]. The advantage of the use of ^{31}P-NMR consists in the opportunity to observe separate signals for both components of the mixture. This allows an analysis of the phase behaviour and mobility of the individual phospholipid components. This method was used to derive a phase diagram of the DPPC-DPPE mixture. On the basis of an approach given by Lee [3,15] a phase diagram was calculated assuming non-ideal mixing of the components. We show that the experimental and theoretical phase diagrams can be analysed to give information about the properties of the mixture.

Abbreviations: DMPC, dimyristoyl phosphatidylcholine; DPPC, dipalmitoyl phosphatidylcholine; DPPE, dipalmitoyl phosphatidylethanolamine; DSC, differential scanning calorimetry; ESR, electron spin resonance; SPDE NMR; spin-half pair dipolar echo NMR.

II. Materials and Methods

DPPC from Ferak and DPPE from Fluka were used without further purification. Binary phospholipid

0 005-2736/81/0000–0000/$02.50

mixtures of DPPC and DPPE were prepared by vacuum evaporation of a chloroform-methanol (2 : 1, v/v) solution. Heavy water was added to the phospholipid preparation. The sample tubes were sealed and the contents were compressed by centrifugation. After this the sample tubes were stored for a week at a temperature above the phase transition temperature to ensure complete equilibration of water. This procedure produced homogeneous aqueous phospholipid dispersions.

For the ^{31}P-NMR measurements a Bruker HX-90 spectrometer was used which was equipped with a deuterium lock, temperature control and facilities for strong broad band decoupling of protons (about 600 W).

The anisotropies of chemical shift $\Delta\delta$ were determined from the experimental spectra by fitting the experimental line shapes using line shape calculations. The calculations were performed by a simple superposition of the lamellar line shapes of the individual phospholipid components using the appropriate intensities and $\Delta\delta$ values. The details of such calculations are given in Refs. 11 and 16. In all cases sufficient agreement between experimental and theoretical line shapes could be reached. The calculations are sensitive to variations of $\Delta\delta$ in the order of ±2 ppm.

III. Experimental results

As illustrative examples experimental ^{31}P-NMR spectra of an equimolar mixture of DPPC and DPPE at temperatures of 329 K (liquid-crystalline state) and 317 K (gel state) are shown in Fig. 1. These signals are characteristic of a lamellar phase but a closer inspection of these line shapes demonstrates that the signals consist of two lamellar line shapes with slightly different anisotropies of chemical shift. From the comparison of spectra of samples with different mole fractions of DPPC and DPPE we can conclude that the smaller component is connected with DPPC as indicated in Fig. 1.

In Fig. 2 the temperature dependence of the measured anisotropies of chemical shift of both components is given. We find that the anisotropies of chemical shift $\Delta\delta$ of both components agree at higher temperatures and are similar to those which were measured for the pure DPPC/water

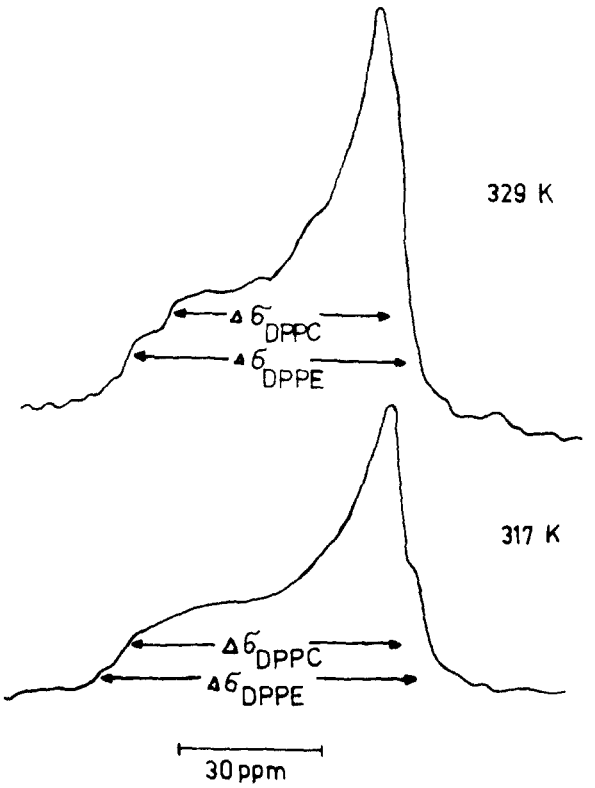

Fig. 1. ^{31}P-NMR spectra of an equimolar mixture of DPPC and DPPE at 329 K and 317 K with proton noise decoupling. Each spectrum consists of two signals which can be characterized by the anisotropies of chemical shift $\Delta\delta_{DPPC}$ and $\Delta\delta_{DPPE}$ as indicated.

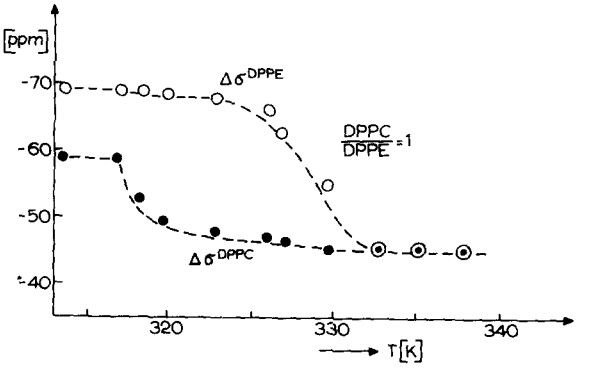

Fig. 2. Temperature dependence of the anisotropy of chemical shift $\Delta\delta$ of the both components of an equimolar mixture of DPPC and DPPE. The broken lines are the calculated temperature dependences of $\Delta\delta_{DPPC}$ and $\Delta\delta_{DPPE}$ as given in the text.

and DPPE/water dispersions (–45 ppm) [17,18]. On lowering the temperature $\Delta\delta$ of DPPE starts to increase at about 331 K but the $\Delta\delta$ value of DPPC is unchanged up to about 319 K. Then the value of DPPC increases from about –47 ppm to about –59 ppm at 317 K within a very small temperature range. The anisotropy of chemical shift of DPPE approaches a value of about –69 ppm.

For all studied mixtures each of the two curves has two abrupt changes of slope which can be interpreted as the onset and the completion of the phase transition of the individual components. The transition temperatures are determined from the intersections of lines drawn through the three main regions of each curve. The breaks of the highest temperature and lowest temperature correspond to a point on the fluidus curve and a point on the solidus curve, respectively, of the phase diagram, e.g. 331 K and 317 K for the equimolar mixture of DPPC and DPPE.

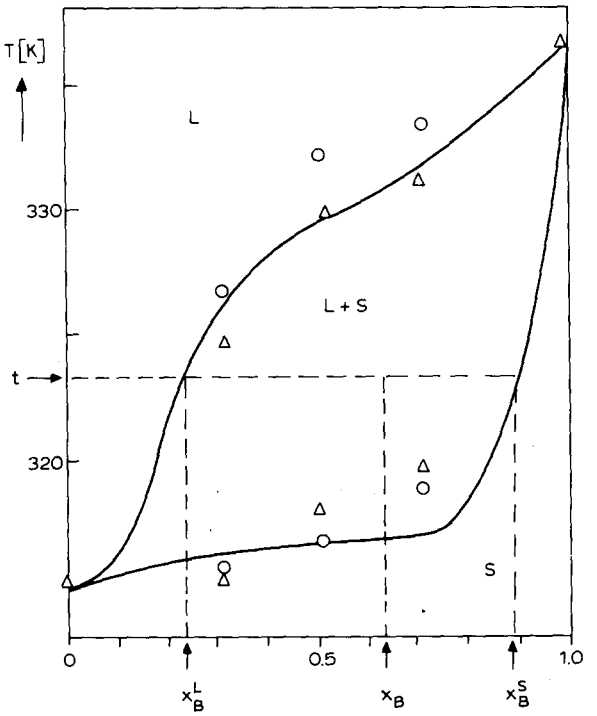

Fig. 3. Phase diagram for mixtures of DPPC and DPPE. ○, determined by ^{31}P-NMR with proton noise decoupling, △, determined from ^{1}H-SPDE NMR measurements. Solid lines are the calculated phase diagram as given in the text (liquidus and solidus curve). L indicates the range of existence of the liquid-crystalline and S that of the solid phase.

In this manner the phase diagram was constructed by studying the variation in $\Delta\delta$ with temperature for three mixtures of different composition and the pure components (Fig. 3). S corresponds to a solid or gel phase and L to a liquid-crystalline or fluid phase state. In Fig. 3 the results of measurements using the ^{1}H-SPDE method [19] are also given. This method provides informations about the motion of the fatty acid chains.

This method of constructing the phase diagram contains an uncertainty in the determination of the onset and completion temperatures of the phase transitions due to the rounded nature of the temperature dependence of the anisotropies of chemical shift and an extrapolation procedure is necessary as given before. Moreover the onset and completion temperatures must be corrected for the contributions to the total transition widths which come from the finite widths of the transitions of the pure lipids. Mabrey and Sturtevant [20] considered this error by increasing the measured onset temperature and decreasing the measured completion temperature by a quantity which depends on the transition widths of the individual lipids.

Because of these difficulties we used the complete temperature dependence of the measured anisotropies of chemical shift (Fig. 2) for the comparison of the experimental behaviour with the calculated phase diagram (see below).

IV. Calculation of the phase diagram

Lee [3,15] has given a thermodynamic approach to the calculation of phase diagrams. For the calculation the melting points T_A and T_B and the heats of melting ΔH_A and ΔH_B of both components A and B are necessary (We assume that A is the lower melting component, i.e. $T_A < T_B$). Then the mole fractions of A and B in the liquid-crystalline state x_A^L and x_B^L and in the solid state x_A^S and x_B^S are given for each temperature T by the following equations [15]:

$$x_A^L = -\exp\left[\ln(1-x_A^S) - \frac{p_0^L(x_A^L)^2 - p_0^S(x_A^S)^2}{RT} - \frac{\Delta H_B}{R}\left(\frac{1}{T} - \frac{1}{T_B}\right)\right] \quad (1)$$

$$x_A^S = \exp\left[-\ln x_A^L + \frac{p_0^L(1-x_A^L)^2 - p_0^S(1-x_A^S)^2}{RT} + \frac{\Delta H_A}{R}\left(\frac{1}{T} - \frac{1}{T_A}\right)\right] \quad (2)$$

The meaning of $x_B^L = (1 - x_A^L)$ and $x_B^S = (1 - x_A^S)$ is given in Fig. 3. Because of their transcendental nature, these equations require numerical methods for their solution and an iteration technique was used [15,16]. These equations contain the constants p_0^L and p_0^S which characterize the nonideal mixing of the two lipids in the mixture [15]. These constants are determined by the best fit of the theoretical phase diagram to the experimental data. For our calculations we used $T_A = 315$ K, $T_B = 337$ K, $\Delta H_A = \Delta H_B = 37.6$ kJ/mol. The experimental phase diagram can be fitted by assuming nonideal mixing in both phases with $p_0^L = 3.8$ kJ/mol and $p_0^S = 5.4$ kJ/mol. The shapes of the calculated phase diagrams are very sensitive to the values of p_0 [16].

As Lee [15] demonstrated the values of p_0^L and p_0^S can be used to obtain the relative distribution of lipids along the plane of the bilayer. At a 1 : 1 molar ratio of A and B the ratio of the probability of finding a molecule of type B next to A to the probability of finding a molecule of type A is given by the following equation

$$\frac{x_{AB}}{x_{AA}} = 2\exp\left(-\frac{p_0}{4RT}\right) - 1 \quad (3)$$

In our case the values for the ratio x_{AB}/x_{AA} are 0.4 for the liquid-crystalline state and 0.2 for the solid state.

V. Calculations of the anisotropies of chemical shift

It should be noted that the experimental points of the phase diagram given in Fig. 3 are only connected with the highest and lowest changes of the slope of the anisotropies of chemical shift. But the special dependences of $\Delta\delta_{DPPC}$ and $\Delta\delta_{DPPE}$ on temperature were not used.

The phase diagram contains all the data needed to calculate the theoretical temperature dependence of the anisotropies of chemical shift. Thus the anisotropies are a very sensitive test of the quality of the constructed phase diagram.

As an example we consider a mixture of the composition x_B at a temperature T within the phase transition range. Then a liquid-crystalline phase with mole fractions x_A^L and x_B^L for A and B is in equilibrium with a solid phase with mole fractions x_A^S and x_B^S (see Fig. 3).

The numbers of molecules in the liquid-crystalline and solid phases, n_L and n_S, are given by the following relation [16]:

$$\frac{n_L}{n_L + n_S} = \frac{x_B^S - x_B}{x_B^S - x_B^L}$$

Because in every case only one signal is observed for each of the components A and B we can assume that the molecules are rapidly exchanged between the liquid-crystalline and solid phase. Therefore we measure an averaged anisotropy of chemical shift $\Delta\delta_A$ and $\Delta\delta_B$ of both components of the mixture. If we consider the partition of molecules the following relations result:

$$\Delta\delta_A = (n_L \cdot x_A^L \cdot \Delta\delta_A^L + n_S \cdot x_A^S \cdot \Delta\delta_A^S)\, x_A^{-1} \quad (5)$$

$$\Delta\delta_B = (n_L \cdot x_B^L \cdot \Delta\delta_B^L + n_S \cdot x_B^S \cdot \Delta\delta_B^S)\, x_B^{-1} \quad (6)$$

Here $\Delta\delta_A^L$, $\Delta\delta_A^S$, $\Delta\delta_B^L$, $\Delta\delta_B^S$ are the anisotropies of the ^{31}P-NMR signals of the A and B molecules in the liquid-crystalline and solid states. For calculations the measured values above and below the phase transition range were used. The calculated temperature dependences of $\Delta\delta_A$ and $\Delta\delta_B$ are given in Fig. 2 (broken lines) for the equimolar mixture of DPPC and DPPE using the constructed phase diagram of Fig. 3. We can see that the theoretical curves fit the measured anisotropies very well.

VI. Discussions

In the electron spin resonance [1], the fluorescence technique [3] and differential scanning calorimetry [2] the variation of one suitable parameter with temperature was studied and two breaks in plots of this parameter were used to find the fluidus and the solidus curve of the phase diagram. But these parameters cannot characterize the melting

behaviour of the single phospholipids of the mixture. By contrast the anisotropies of chemical shift which are connected with the individual components of the mixture provide data about the phase state of each component. Cullis et al. [10] used a similar method to characterize the effect of cholesterol on an equimolar mixture of DPPC and $18:1_c/18:1_c$-PE. From our measurements we can conclude that there is no cocrystallization of DPPC and DPPE of cooling. The temperature dependence of the anisotropies of chemical shift (Fig. 2) demonstrates that at first the DPPE crystallizes and the DPPC crystallization appears at lower temperatures. The DPPC and DPPE molecules are separated into different regions. The same behaviour was found for a sonicated DPPC-DPPE mixture before by observing the temperature dependence of the ^{31}P-NMR line widths [4] of the DPPC and DPPE signals of the mixture.

The general good agreement between the experimental and the theoretical temperature dependence of the anisotropies of chemical shift gives some reason for confidence in the reality of the values of the parameter p_0 describing the non-ideality of mixing. The calculated value of 2.5 for x_{AA}/x_{AB} very strongly suggests that a nonrandom distribution of DPPC and DPPE molecules can be expected even in the liquid-crystalline phase. This means that the interaction between two like molecules is stronger than the interaction between two unlike molecules. The studied phospholipids have the same fatty acyl chains. Therefore this difference is probably caused by the headgroups, so that the interaction between unlike headgroups is weaker.

The cluster-like organization of a similar lipid mixture of DMPC and DMPE has been verified by electron microscopy [21]. It was found that fluid DMPC coexists with crystalline DMPE at temperaturs between the phase transition temperatures of the isolated components. The diameter of the clusters was estimated to vary between 500 and 1000 Å. There is no doubt that electron microscopy gives the best view of a lipid domain and the most accurate size of the domain, but it is very largely restricted to a static picture of a domain. A special property of our results is the fast exchange of the DPPE and DPPC molecules between the liquid-crystalline and solid regions in the temperature range of the phase transition. This fast exchange of molecules results in an averaging of the anisotropies of chemical shift of each of the components.

These results are of importance for the interpretation of the ^{31}P-NMR spectra of more complex systems such as lipid-protein systems and biological membranes. In most cases the exchange of boundary lipid with the bulk lipid is fast enough to average the anisotropy of chemical shift of the ^{31}P-NMR signal and no separate signals are observed for the two forms of lipids. This is confirmed by measurements of Cullis and Grathwohl [22] on erythrocyte membranes and Seelig and Seelig [23] on reconstituted cytochrome *c* oxidase/phospholipid membranes.

References

1 Shimshick, E.J. and McConnell, H.M. (1973) Biochemistry 12, 2351–2360
2 Blume, A. and Ackermann, T. (1974) FEBS Lett. 43, 71–74
3 Lee, A.G. (1975) Biochim. Biophys. Acta 413, 11–23
4 Arnold, K., Frischleder, H. and Klose, G. (1976) Wiss. Z. Karl-Marx-Univ. Leipzig 25, 615–624
5 Lee, A.G. (1977) Biochim. Biophys. Acta 472, 285–344
6 Fockson, J.E., Wallach, D.F.H. (1978) Arch. Biochem. Biophys. 189, 195–204
7 Luna, E.J. and McConnell, H.M. (1978) Biochim. Biophys. Acta 509, 412–423
8 Cullis, P.R. and De Kruijff, B. (1978) Biochim. Biophys. Acta 513, 31–42
9 Cullis, P.R. and De Kruijff, B. (1978) Biochim. Biophys. Acta 507, 207–218
10 Cullis, P.R., Van Dijck, P.W.M., De Kruijff, B. and De Gier, J. (1978) Biochim. Biophys. Acta 513, 21–30
11 Arnold, K., Gawrisch, K. and Volke, F. (1979) Stud. Biophys. 76, 85–93
12 Seelig, J. and Gally, H. (1976) Biochemistry 15, 5199–5204
13 Frenzel, J., Arnold, K. and Nuhn, P. (1978) Biochim. Biophys. Acta 507, 185–197
14 Arnold, K., Lösche, A. and Gawrisch, K. (1981) Stud. Biophys., in the press
15 Lee, A.G. (1978) Biochim. Biophys. Acta 507, 433–444
16 Lösche, A. (1979) Thesis, Leipzig
17 Gawrisch, K., Arnold, K., Rüger, H.-J., Kertscher, P. and Nuhn, P. (1977) Chem. Phys. Lipids 20, 285–292
18 Seelig, J. (1978) Biochim. Biophys. Acta 515, 105–140
19 Boden, N., Jackson, P., Levine, Y.K. and Ward, A.J.I. (1976) Biochim. Biophys. Acta 419, 395–403

20 Mabrey, S. and Sturtevant, J.M. (1976) Proc. Natl. Acad. Sci. U.S.A. 73, 3862–3866
21 Sackmann, E. (1978) Ber. Bunsenges. Phys. Chem. 82, 891–909
22 Cullis, P.R. and Grathwohl, C. (1977) Biochim. Biophys. Acta 471, 213–226
23 Seelig, A. and Seelig, J. (1978) Hoppe Seylers Z. Physiol. Chem. 359, 1747–1756